

High-quality fiber Bragg grating inscribed in ZBLAN fiber using femtosecond laser point-by-point technology

LIN CHEN,^{1,2} CAILING FU,^{1,2,*} ZIHAO CAI,^{1,2} PENGSHENG SHEN,^{1,3} YU FAN,^{1,2} HUAJIAN ZHONG,^{1,2} CHAO DU,^{1,2} YANJIE MENG,^{1,2} YIPING WANG,^{1,2} CHANGRUI LIAO,^{1,2} JUN HE,^{1,2} AND WEIJIA BAO^{1,2}

¹Key Laboratory of Optoelectronic Devices and Systems of Ministry of Education and Guangdong Province, College of Physics and Optoelectronic Engineering, Shenzhen University, Shenzhen 518060, China

²Shenzhen Key Laboratory of Photonic Devices and Sensing Systems for Internet of Things, Guangdong and Hong Kong Joint Research Centre for Optical Fibre Sensors, Shenzhen University, Shenzhen 518060, China

³Shenzhen Key Laboratory of Laser Engineering, Guangdong Provincial Key Laboratory of Micro/Nano Optomechatronics Engineering, Shenzhen University, Shenzhen 518060, China

*Corresponding author: fucailing@szu.edu.cn

Received 13 May 2022; revised 22 June 2022; accepted 23 June 2022; posted 23 June 2022; published 7 July 2022

We demonstrate for the first time, to the best of our knowledge, the fabrication of a high-quality fiber Bragg grating (FBG) in ZBLAN fiber by using an efficient femtosecond laser point-by-point technology. Two types of FBG, e.g., high coupling coefficient and narrow bandwidth grating, are successfully obtained. The coupling coefficient is strongly dependent on the grating order and pulse energy. A second-order FBG with an ultrahigh coupling coefficient of 325 m^{-1} and reflectivity of 97.8% is inscribed in the ZBLAN fiber. A pair of FBGs with a narrow FWHM of 0.30 and 0.09 nm are also demonstrated. © 2022 Optica Publishing Group

<https://doi.org/10.1364/OL.464006>

A mid-infrared fiber laser has versatile applications in optical communication [1], remote sensing [2], and molecular detection [3]. A key component of the mid-infrared fiber laser is the fiber Bragg grating (FBG) inscribed in fluoride glass fiber, which could be used as in-fiber mirrors to realize the output of the high-power laser without calibration [4–6]. Femtosecond laser inscription technology is promising for inscribing the FBG in a passive or active ZBLAN glass fiber due to its ultrashort pulse duration and ultrahigh peak intensity [7]. Recently, various methods based on a femtosecond laser have been proposed and demonstrated to inscribe FBGs in a fluoride glass ZBLAN fiber [8–13]. Bernier *et al.* demonstrated the inscription of an FBG in both Tm-doped and undoped ZBLAN fibers by using a femtosecond laser and a phase mask [8]. Note that the polymer coating of the fiber was removed prior to inscribing the FBG. Subsequently, using this method, a pair of FBGs in an Er-doped fluoride fiber without removing the coating was successfully employed to emit a maximum average output power of 11.2 W at 2.826 μm [9]. However, the phase mask inscription method based on a femtosecond laser requires using a phase mask with a specific period, which makes the method relatively inflexible [14].

Compared with the phase mask inscription method, the femtosecond laser direct-writing method exhibits good flexibility in the selection of grating period, order, length, and wavelength [10–12]. Goya *et al.* demonstrated the inscription of a 2.4-mm-FBG in an Er-doped fluoride fiber by using femtosecond laser plane-by-plane technology, realized by scanning the fiber in the Y and Z directions across the fiber core at a constant velocity, where the total fabrication time was 90 min [10]. Then the single pass, double pass, and stacking method based on femtosecond laser plane-by-plane technology was also demonstrated and analyzed to obtain a 5-mm third-order FBG with a high coupling coefficient, where the total fabrication time was approximately 2.5, 5.0, and 7.0 h, respectively [11]. As we know, the plane-by-plane technology is based on the line-by-line technology. Compared with the fabrication time of several hours for line-by-line and plane-by-plane technology, the point-by-point technology requires typically less than a minute for inscribing an FBG at a repetition rate of the inscription laser of 1 kHz [15]. Unfortunately, the inscription of an FBG in a fluoride glass ZBLAN fiber by use of femtosecond laser point-by-point technology has not been reported since 2013 [12].

In this Letter, we experimentally report for the first time, to the best of our knowledge, the fabrication of a high-quality FBG in ZBLAN fiber by use of femtosecond laser point-by-point technology. Matching oils with a different refractive index are investigated to generate a smooth refractive index modification. Moreover, the dependence of the coupling coefficient for the FBG on the grating order and pulse energy are investigated to obtain an FBG with a higher coupling coefficient, i.e., higher reflectivity. Furthermore, the bandwidth, i.e., full width at half maximum (FWHM), property of the obtained FBG is also studied.

As shown in Fig. 1, a femtosecond laser (Pharos, Light-Conversion) with a pulse width of 290 fs, central wavelength of 514 nm, and repetition rate of 200 kHz was employed to inscribe an FBG in the ZBLAN fiber by using point-by-point

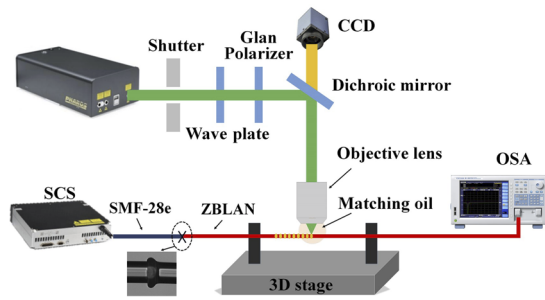


Fig. 1. Experimental setup for fabricating fiber Bragg gratings (FBGs) in ZBLAN fiber using femtosecond laser point-by-point technology. SCS, supercontinuum source; OSA, optical spectrum analyzer.

technology. The core/cladding diameter, cutoff wavelength, and numerical aperture (NA) of the passive ZBLAN fiber (Le Verre Fluoré) was 6.5/125 μm , 1.95 μm , and 0.23, respectively. A shutter was used to open/close the femtosecond laser beam. A variable attenuator composed of a wave plate and a Glan-prism polarizer was used to adjust the energy and polarization of the laser. A dichroic mirror was used to reflect the femtosecond laser to the objective lens and transmit the visible illumination beam to the CCD. With the assistance of the CCD, the femtosecond laser was focused on the core of the ZBLAN fiber through a 100 \times oil-immersion objective lens, where the NA was 1.32. The ZBLAN fiber was fixed by a pair of fiber holders mounted on an assembled 3D high-precision air-bearing translation stage (Aerotech ABL15010, ANT130LZS, and ANT130V-5). Note that the fiber coating was not stripped off before FBG inscription. In the experiment, position synchronized output was employed to accurately control the output of the single pulse laser to realize the femtosecond laser point-by-point technology, i.e., a pulse was a modulation point. The fiber was moved along the fiber axis with a constant velocity of V , i.e., $V = 200 \mu\text{m/s}$, and then a series of modulation points were induced in the fiber core, i.e., obtaining an FBG in the ZBALN fiber. Compared with femtosecond laser line-by-line technology [11], only 100 s would be needed to fabricate an FBG with a length of 20 mm using point-by-point technology. Note that the ZBLAN fiber, i.e., fluoride glass fiber, was spliced to SMF-28e with an automated glass processor workstation (Vytran GPX-3000, Thorlabs).

To minimize the geometric aberration of the femtosecond laser beam in the cylindrical fiber, i.e., ZBLAN fiber, different types of matching oils, i.e., refractive index of 1.498, 1.480, 1.474, and 1.464, were applied between the objective lens and ZBLAN fiber. As shown in Figs. 2(a)–2(c), the shape of modulation points in the ZBLAN fiber induced by femtosecond laser

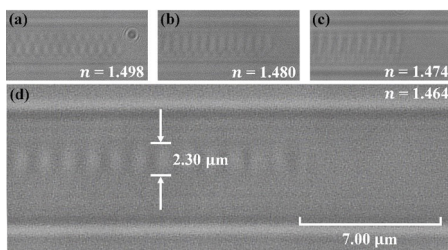


Fig. 2. Lateral view microscopy images of modulation points induced by matching oil with the refractive index of (a) 1.498, (b) 1.480, (c) 1.474, and (d) 1.464 in the ZBLAN fiber.

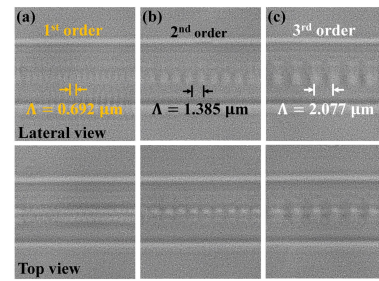


Fig. 3. Lateral and top view of short structures for (a) first-, (b) second-, and (c) third-order FBG in a ZBLAN fiber fabricated with a laser energy of 30 nJ.

point-by-point technology became more regular and smoother, i.e., the aberration was gradually minimized, with the decrease of the refractive index of the matching oil. As shown in Fig. 2(d), the most regular and smooth modulation points with a focal depth of 2.3 μm were observed when the refractive index of the matching oil was decreased to 1.464. When the refractive index of the matching oil was further decreased, the shape of the modulation point remained unchanged, but a higher pulse energy was required to obtain the FBG. Therefore, the matching oil with a refractive index of 1.464 was finally selected to generate a smooth refractive index modification to minimize the aberration.

It is well known that the Bragg wavelength, i.e., λ_B , of the FBG in the ZBLAN fiber based on coupled-mode theory is given by

$$\lambda_B = \frac{2n_{\text{eff}}\Lambda}{m}, \quad (1)$$

where n_{eff} is the effective modal refractive index of the propagating mode, and Λ and m are the period and order of the FBG. The reflectivity, i.e., R , of the FBG in the ZBLAN fiber is given by

$$R = \tanh^2(\kappa L), \quad (2)$$

where L is the length of FBG and κ is the coupling coefficient between two counter-propagating guided modes, which is given by

$$\kappa = \frac{\pi \Delta n \eta}{\lambda_B}, \quad (3)$$

where Δn is the refractive index modulation induced by the femtosecond laser and η is the factor of the mode overlap.

To investigate the effect of the grating order on the coupling coefficient, i.e., κ , under the same length, three types of FBGs with different orders, i.e., $m = 1, 2,$ and 3 , were inscribed in the ZBLAN fiber, where the periods of first-, second-, and third-order FBG were set to 0.692, 1.385, and 2.077 μm , respectively. As shown in Figs. 3(b) and 3(c), each period, i.e., each modulation point induced by the femtosecond laser point-by-point technology, of the second- and third-order FBG could be clearly observed and distinguished, while that of the first-order was difficult to distinguish resulting from the overlapping of adjacent periods caused by the small period, i.e., 0.692 μm , as shown in Fig. 3(a). Note that the fabrication pulse laser energy was 30 nJ. As shown in Fig. 4(a), the coupling attenuation, i.e., reflectivity, of the first-order FBG was gradually increased, when the grating length was increased from 2 to 8 mm with a step of 2 mm. A supercontinuum source (SCS) with a wavelength of 480–2200 nm, and an optical spectrum analyzer (OSA) with a

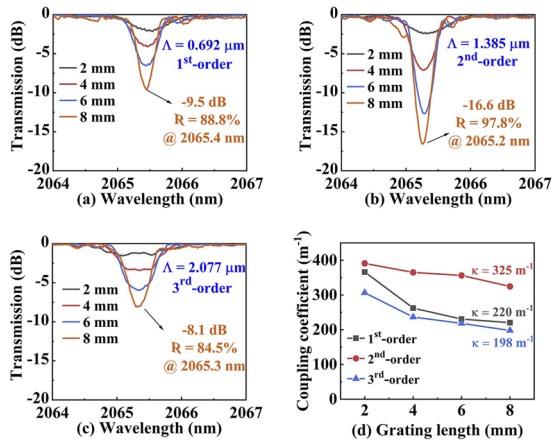


Fig. 4. Transmission spectra of (a) first-order, (b) second-order, and (c) third-order FBG in a ZBLAN fiber under the same pulse energy, i.e., 30 nJ, where the periods of the first-, second-, and third-order grating are 0.692, 1.385, and 2.077 μm , respectively; (d) coupling coefficient, i.e., κ , of the first-, second-, and third-order FBG as a function of the grating length, i.e., L , labeled by black, red, and blue curves, respectively.

resolution of 0.05 nm were employed to measure the transmission spectrum of the FBG in the ZBLAN fiber. The second- and third-order FBG exhibited the same trend as the first-order FBG inscribed in the ZBLAN fiber, as shown in Figs. 4(b) and 4(c). When the length of the first-, second-, and third-order FBG was 8 mm, the Bragg wavelength and coupling attenuation were (2065.4 nm, -9.5 dB), (2065.2 nm, -16.6 dB), and (2065.3 nm, -8.1 dB), corresponding to the reflectivity of 88.8%, 97.8%, and 84.5%, respectively. According to the reflectivity, i.e., R , and length of the FBG, i.e., L , the coupling coefficient, i.e., κ , could be calculated using Eq. (1) under the length of 2, 4, 6, and 8 mm. As shown in Fig. 4(d), the coupling coefficient of first-, second-, and third-order FBG was decreased with the increase of the FBG length. Compared with the first- and third-order FBG, the coupling coefficient of the second-order FBG was the highest regardless of the grating length. Moreover, the coupling coefficient of second-order FBG was 325 m^{-1} , while that of the first- and third-order FBG was 220 and 198 m^{-1} under the grating length of 8 mm.

To investigate the effect of the pulse energy on the coupling coefficient, different pulse energies, i.e., 27, 30, and 32 nJ, were employed to fabricate three second-order FBGs in the ZBLAN fiber with a period of 1.385 μm , i.e., FBG₁, FBG₂, and FBG₃. As shown in Figs. 5(a)–5(c), the reflectivity, i.e., coupling attenuation, of the FBG₁, FBG₂, and FBG₃ was also gradually increased to 83.8%, 97.8%, and 94.4%, when the grating length was increased from 2 to 8 mm. As shown in Fig. 5(d), the coupling coefficients of the FBG₁, FBG₂, and FBG₃ were not a constant with the increase of grating length, which is different from the simulation [16]. It is obvious that the coupling coefficient of the FBG₃ prepared with pulse energy of 32 nJ was not higher than that of FBG₂ prepared with a pulse energy of 30 nJ, but lower than that of FBG₂. As shown in Fig. 5(d), the coupling coefficient of the FBG₂, i.e., 325 m^{-1} , was higher than that of FBG₁ and FBG₃, i.e., 195 and 264 m^{-1} , when the grating length was 8 mm. Moreover, the coupling coefficient of the FBG₂ was higher than that of FBG₁ and FBG₃ regardless of the grating length, and that of FBG₁ was the lowest. This indicated that the

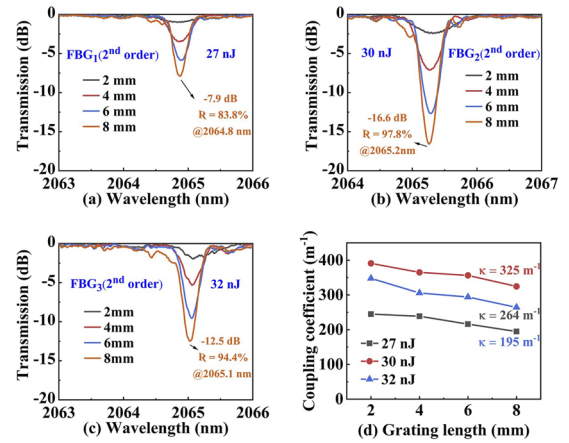


Fig. 5. Transmission spectra of three second-order FBGs, i.e., (a) FBG₁, (b) FBG₂, (c) FBG₃ with a period of 1.385 μm , where the fabrication pulse energies are 27, 30, 32 nJ, respectively; (d) coupling coefficient, i.e., κ , of the FBG₁, FBG₂, and FBG₃ as a function of the grating length, i.e., L , labeled by black, blue, and red, respectively.

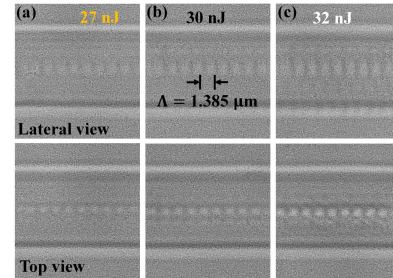


Fig. 6. Lateral and top view microscopy images of short structures for three second-order FBGs i.e., (a) FBG₁, (b) FBG₂, and (c) FBG₃ fabricated with pulse energy of 27, 30, and 32 nJ, respectively, where the period is 1.385 μm .

optimal pulse energy to obtain a second-order FBG with high coupling coefficient was 30 nJ. As shown in Figs. 6(a) and 6(c), the modulation points of the FBG₁ and FBG₃ were too weak and too strong, respectively, while that of FBG₂ was just right, as shown in Fig. 6(b). This confirms again that the optimal pulse energy for the second-order FBG with high coupling coefficient was 30 nJ.

To investigate the bandwidth property of the second-order FBG, the length of the afore-fabricated three second-order FBGs, i.e., FBG₁, FBG₂, and FBG₃, were further increased. When the same reflectivity, i.e., $R \approx 98\%$, of the FBG₁, FBG₂, and FBG₃ was achieved, the grating length, i.e., L , was 20, 10, and 16 mm, and the corresponding coupling coefficient, i.e., κ , was 137, 290, and 170 m^{-1} , respectively. As shown in Table 1, the FWHM of FBG₁, FBG₂, and FBG₃ was 0.299, 0.501, and

Table 1. Characteristics of Three Second-order FBGs Fabricated with Different Energy

FBG	E/nJ	L/mm	$R/\%$	λ_B/nm	FWHM/nm	κ/m^{-1}
FBG ₁	27	20	98.4	2065	0.299	137
FBG ₂	30	10	98.8	2065	0.501	290
FBG ₃	32	16	98.3	2065	0.442	170

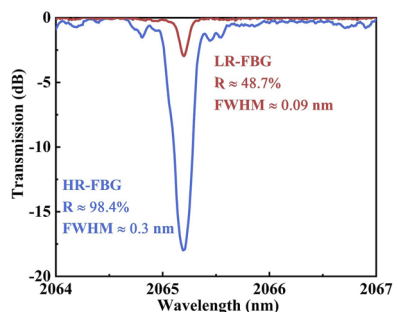


Fig. 7. Transmission spectra of high-reflectivity FBG, i.e., HR-FBG, and low-reflectivity FBG, i.e., LR-FBG, pairs with a narrow FWHM of 0.09 and 0.30 nm, where the reflectivity is 48.7% and 98.4%, respectively.

0.442 nm, indicating a lower pulse energy, i.e., E , resulted in a narrower FWHM. Thus, a pair of FBGs consisted of a high-reflectivity FBG, i.e., HR-FBG, and a low-reflectivity FBG, i.e., LR-FBG, were fabricated in the ZBLAN fiber. As shown in Fig. 7, the FWHM of the HR-FBG was 0.30 nm, where the pulse energy was 27 nJ. When the pulse energy was decreased to 20 nJ, the FWHM of the LR-FBG was narrowed to 0.09 nm, which is the narrowest FWHM in the ZBLAN FBG [13]. The insertion loss was approximately 0.17 dB of the LR-FBG by comparing the transmission spectrum of the grating to that of an unmodified fiber of the same length as a reference. Such FBG pairs have a good application prospect in a single-frequency narrow linewidth fiber laser.

In conclusion, we have proposed and demonstrated an efficient method, i.e., femtosecond laser point-by-point technology, to fabricate a high-quality FBG in a ZBLAN fiber. A matching oil with a refractive index of 1.464 was selected to generate a smooth refractive index modification. Compared with the first- and third-order FBG, the coupling coefficient of the second-order FBG was the highest. Using the optimal pulse energy, i.e., 30 nJ, the second-order FBG with an ultrahigh coupling coefficient of 325 m^{-1} in the ZBLAN fiber could be obtained, where the reflectivity was 97.8%. Moreover, a HR-FBG and LR-FBG with a narrow FWHM of 0.30 and 0.09 nm were also demonstrated. Such a high-quality FBG has the potential in the field of the mid-infrared fiber laser. In addition, such a method, i.e., the femtosecond laser point-by-point technology, is more

suitable for inscribing the FBG in a ZBLAN fiber with a small core diameter, but not suitable for a large diameter fiber due to its small modulation point.

Funding. National Natural Science Foundation of China (61905155, U1913212); Natural Science Foundation of Guangdong Province (2019A1515011393, 2019B1515120042, 2021A1515011925); Science and Technology Innovation Commission of Shenzhen (20200810121618001, JCYJ20200109114020865, JCYJ20200109114201731, JSGG20201102152200001).

Disclosures. The authors declare no conflicts of interest.

Data availability. Data underlying the results presented in this paper are not publicly available at this time but may be obtained from the authors upon reasonable request.

REFERENCES

1. T. J. Carrig and A. M. Schober, *IEEE Photonics J.* **2**, 207 (2010).
2. A. Schliesser, N. Picqué, and T. W. Hänsch, *Nat. Photonics* **6**, 440 (2012).
3. Z. H. Wang, B. Zhang, J. Liu, Y. F. Song, and H. Zhang, *Opt. Laser Technol.* **132**, 20 (2020).
4. F. Maes, V. Fortin, M. Bernier, and R. Vallee, *Opt. Lett.* **42**, 2054 (2017).
5. G. Bharathan, R. I. Woodward, M. Ams, D. D. Hudson, S. D. Jackson, and A. Fuerbach, *Opt. Express* **25**, 30013 (2017).
6. M. R. Majewski, G. Bharathan, A. Fuerbach, and S. D. Jackson, *Opt. Lett.* **46**, 600 (2021).
7. S. Gross, M. Dubov, and M. J. Withford, *Opt. Express* **23**, 7767 (2015).
8. M. Bernier, D. Faucher, R. Vallée, A. Salimnia, G. Androz, Y. Sheng, and S. L. Chin, *Opt. Lett.* **32**, 454 (2007).
9. P. Paradis, V. Fortin, Y. O. Aydin, R. Vallee, and M. Bernier, *Opt. Lett.* **43**, 3196 (2018).
10. K. Goya, H. Matsukuma, H. Uehara, S. Hattori, C. Schafer, D. Konishi, M. Murakami, and S. Tokita, *Opt. Express* **26**, 33305 (2018).
11. G. Bharathan, T. T. Fernandez, M. Ams, R. I. Woodward, D. D. Hudson, and A. Fuerbach, *Opt. Lett.* **44**, 423 (2019).
12. D. D. Hudson, R. J. Williams, M. J. Withford, and S. D. Jackson, *Opt. Lett.* **38**, 2388 (2013).
13. V. Fortin, F. Jobin, M. Larose, M. Bernier, and R. Vallee, *Opt. Lett.* **44**, 491 (2019).
14. S. J. Mihailov, C. W. Smelser, P. Lu, R. B. Walker, D. Grobncic, H. Ding, G. Henderson, and J. Unruh, *Opt. Lett.* **28**, 995 (2003).
15. A. Fuerbach, G. Bharathan, and M. Ams, *IEEE Photonics J.* **11**, 1 (2019).
16. T. Erdogan, *J. Lightwave Technol.* **15**, 1277 (1997).